Effect of Microbial Stimuli and Bone Morphogenetic Protein 2 on Ectopic Bone Formation

Rahmani, Nada Ristya; Duits, Anneli; Khokhani, Paree; Croes, Michiel; Kaludjerovic, Vela; Gawlitta, Debby; Weinans, Harrie; Kruyt, Moyo C.

DOI
10.1089/ten.tea.2025.0020

Publication date
2025

Document Version
Final published version

Published in
Tissue Engineering - Part A

TISSUE ENGINEERING: Part A
Volume 00, Number 00, 2025

DOI: 10.1089/ten.tea.2025.0020

termis
Tissue Engineering
& Regenerative Medicine
International Society

Open camera or QR reader and scan code to access this article and other resources online.

ORIGINAL ARTICLE

Effect of Microbial Stimuli and Bone Morphogenetic Protein 2 on Ectopic Bone Formation

Nada Ristya Rahmani, MD,[1,2] Anneli Duits, MD,[1,2] Paree Khokhani, PhD,[1,2] Michiel Croes, PhD,[1] Vela Kaludjerovic,[1] Debby Gawlitta, PhD,[2,3] Harrie Weinans, PhD,[1,4] and Moyo C. Kruyt, MD, PhD[1,5]

Advancements in biomaterials design increasingly focus on material–host immune interactions as one of the strategies to promote new bone formation, referred to as osteoimmunomodulation. Recent studies indicate that inflammatory stimuli can synergize with growth factors such as bone morphogenetic protein 2 (BMP-2) to promote bone formation. Pathogen-associated molecular patterns (PAMPs) are motifs expressed by microbes that are recognized by immune cells and induce an immune-stimulatory response. In this study, we combined PAMPs with low-dose BMP-2 on a biphasic calcium phosphate (BCP) scaffold and evaluated its effect on ectopic bone formation in a subcutaneous implantation model. The PAMPs tested include gamma-irradiated whole microbes (γi-*Staphylococcus aureus* and γi-*Candida albicans*), a vaccine (Bacillus Calmette-Guérin containing *Mycobacterium bovis*), bacterial cell wall components (peptidoglycan [PGN], lipopolysaccharide [LPS], lipoteichoic acid, and Pam3CysSerLys4), an exopolysaccharide (Curdlan), and nucleic acid analogues (polyinosinic:polycytidylic acid [Poly(I:C)] and Cytidine–phosphate–guanosine [CpG]-containing oligonucleotides type C). Implants consisting of BCP, PAMPs, and BMP-2 were placed subcutaneously in rabbits and evaluated for ectopic bone formation after 5 weeks. Implants with only BMP-2 served as controls. Of the PAMPs tested, only PGN and BMP-2 showed a positive bone volume compared with the control, with borderline significance (+4.4%, $p = 0.08$). Decreased bone volume was seen for LPS (−7.4%, $p = 0.03$) and Poly(I:C) (−6.3%, $p = 0.04$). Fluorochrome labeling at weeks 2 and 3 assessed mineralization onset, revealing no mineralization in the first 2 weeks and some implants showing onset at week 3. We observed variability in ectopic bone formation across animals, associated with higher osteoclast numbers in those where ectopic bone occurred versus those that did not ($p = 0.004$). PAMPs can modulate bone formation, but their effects are variable, requiring further refinement to harness their osteoimmunomodulatory properties effectively. Additionally, we highlight osteoclasts' important role in stimulating ectopic bone formation.

Keywords: osteoimmunomodulation, bone regeneration, PAMPs, osteoclast, *in vivo*, rabbit

Impact Statement

Immune mediators have been shown to modulate both bone formation and bone loss. Pathogen-associated molecular patterns (PAMPs) are potent immunomodulators that elicit a wide range of immune-stimulatory responses. To determine whether PAMPs potentially function for osteoimmunomodulation to promote bone formation, we combined bone-substitute material

[1]Department of Orthopedics, University Medical Center Utrecht, Utrecht, The Netherlands.
[2]Regenerative Medicine Center Utrecht, University Medical Center Utrecht, Utrecht University, Utrecht, The Netherlands.
[3]Department of Oral and Maxillofacial Surgery, Prosthodontics & Special Dental Care, University Medical Center Utrecht, Utrecht, The Netherlands.
[4]Department of Biomechanical Engineering, Technical University Delft, Delft, The Netherlands.
[5]Department of Developmental Biomedical Engineering, Twente University, Enschede, The Netherlands.

with different PAMPs and low-dose bone morphogenetic protein 2 (BMP-2). Implants were tested in a challenging extraskeletal (ectopic) implantation model and evaluated for *de novo* bone formation. We saw a minimal effect of PAMPs on ectopic bone formation for most PAMPs tested in our model. Only peptidoglycan, a prominent bacterial cell wall component, in combination with BMP-2 resulted in a positive bone volume compared with BMP-2-only controls, with borderline significance. Future studies using more predictive *in vivo* models are needed to evaluate the potential of PAMPs as osteoimmunomodulatory agents. Additionally, our results suggest osteoclasts to be associated with differences in ectopic bone formation across animals and therefore a relevant parameter to be included in future studies using ectopic implantation models.

Introduction

Bone is a specialized form of connective tissue that protects vital organs, supports load transfer during movement, provides a reservoir for minerals, and is the source of blood cells.[1] It can self-regenerate; however, conditions such as large defects surpass this natural capacity, leading to disruptions in the skeletal system that can significantly diminish the quality of life.[2] The current gold standard for managing bone defects, autografting, involves harvesting bone and transplanting within the patient's body. Yet, this approach is constrained by limited supply and necessitates additional surgical procedures.[3] Therefore, an off-the-shelf bone graft substitute replicating, for instance, the bone tissue's inorganic component presents a valuable alternative.

Efforts are increasingly focused on developing bone graft substitutes that not only serve a structural purpose but also have bioactive properties, enabling stimulation of new bone formation.[4] One such strategy is rendering the biomaterials with immune-modulating properties, referred to as osteoimmunomodulation.[5] Recent research has demonstrated that bacterial ligands can trigger a biological response that promotes the formation of new bone tissue, likely through modulation of the immune response.[6–8] For instance, the direct injection of irradiated *Staphylococcus aureus* and *Escherichia coli* into the tibial canal of rabbits triggered significant thickening of the bone cortex, with signs of healthy new bone tissue formation.[6]

The unconventional approach of using microbial stimuli as a therapeutic strategy is supported by the clinical observation that patients with osteomyelitis present symptoms of both bone lysis and bone growth.[9] Bone lysis typically occurs near the infection site, while in the periphery of the infection, sporadic bone growth can occur.[9] Moreover, acquired bone formation in soft tissues can develop as in the pathogenesis of heterotopic ossification, which involves repeated exposure to inflammatory stimuli, heightened sensitivity to bone morphogenetic protein 2 (BMP-2), and precipitation of calcium ions.[10,11] Given the tight connection between the activation of the immune system and bone formation, modulation of one system can affect the other. Nonetheless, there appears to be a specific range, in which inflammatory conditions can promote bone formation rather than hinder it.[12] Harnessing inflammation can therefore be a strategy to render bone graft substitutes with bioactive properties.

Microbes express molecular motifs that immune cells recognize.[13] These motifs are collectively known as pathogen-associated molecular patterns (PAMPs) and can bind to immune cells via pattern recognition receptors (PRRs). PRRs are expressed on cell membranes and in their cytoplasm, allowing constant surveillance of pathogens. When PAMPs bind to PRRs, a series of signaling cascades is triggered inside the cells resulting in the secretion of inflammatory mediators.[13] Different PAMPs induce different immune responses, and therefore, it is intriguing to investigate which types of PAMPs can modulate an immune response that benefits bone formation.

This study investigates the application of various PAMPs on ectopic bone formation in a biphasic calcium phosphate (BCP) scaffold. The PAMPs tested include gamma-irradiated whole microbes (γi-*Staphylococcus aureus* [SA] and γi-*Candida albicans* [CA]), a vaccine (Bacillus Calmette-Guérin [BCG] containing attenuated *Mycobacterium bovis*), various bacterial cell wall components (peptidoglycan [PGN], lipopolysaccharide [LPS], lipoteichoic acid [LTA], and Pam3CysSerLys4 [PAM]), an exopolysaccharide (Curdlan), and analogs of microbial nucleic acids (polyinosinic:polycytidylic acid [Poly(I:C)] and CpG-containing oligonucleotides type C [CpG ODN C]). Based on the previous studies using extraskeletal (ectopic) implantation models in rabbits,[7,12,14] we combined the inflammatory stimuli with a low dose of BMP-2 in porous BCP scaffolds. By adding an osteogenic factor such as BMP-2 at a low dose, we can observe the effect of PAMPs on bone formation in two directions: inhibition or promotion.

Materials and Methods

Materials

Whole microbes were obtained from the microbiology department of the University Medical Center Utrecht, the Netherlands. *S. aureus* (Wood 46, ATCC 10832) was cultured in lysogeny broth medium at 37°C to midlog phase, and *C. albicans* (ATCC 10231) was cultured in malt agar medium (OD_{660} 1.0). The microbes were made nonviable by exposure to gamma irradiation (γi) at 25 kGy (Steris AST, Ede, the Netherlands) and stored at −80°C in phosphate-buffered saline (PBS) with 40% (v/v) glycerol. Attenuated *M. bovis* in the form of BCG vaccine (Medac, Lamepro B.V., The Netherlands) was obtained from the University Medical Center Utrecht pharmacy. Peptidoglycan (PGN-SAndi ultrapure peptidoglycan), polyinosinic:polycytidylic acid high molecular weight, CpG oligodeoxynucleotide type C (M362), PAM, Curdlan (beta-1,3-glucan from *Alcaligenes faecalis*), LPS (from *E. coli* O55:B5), and LTA (purified from *S. aureus*) were purchased from Invivogen (France).

The ceramic scaffold employed was commercially available BCP in the shape of discs (6 × 9 mm Ø) comprising 65–75% tricalcium phosphate [$Ca_3(PO_4)_2$] and 25–35% hydroxyapatite

$[Ca_{10}(PO_4)_6(OH)_2]$ (MagnetOs; Kuros Biosciences BV, Switzerland). The discs had a porosity of ±75% with submicron (<3 μm) needle-shaped surface topography.[15]

Determining PAMP concentration using a whole blood assay

To determine the working concentration of PAMPs to add to the implants, we initially assessed the rabbits' immune response toward different concentrations of PAMPs. A whole blood assay was conducted following a previously reported protocol.[16] Briefly, sterile blood was collected ($n = 5$ rabbits) in a sodium heparin-coated tube and then diluted 5× with medium containing RPMI (1640, Gibco, Sigma-Aldrich, USA) and 100 U/mL penicillin and 100 U/mL streptomycin (Gibco, Sigma-Aldrich). PAMPs (0.01, 0.1, 1, and 10 μg/mL) were added to the diluted blood and then incubated for 24 h at 37°C and 5% carbon dioxide. Supernatants were collected and measured for interleukin (IL) 6 using the Rabbit DuoSet® ELISA kit (R&D Systems, the Netherlands) following the manufacturer's protocol. IL-6 was chosen as a general indicator of a proinflammatory response. Results of the whole blood assay are depicted in Supplementary Figure S1.

Specifically, for LPS and LTA, the concentrations used (100 μg/mL and 3 mg/mL, respectively) were based on a previous study.[7]

Implant preparation

BCP discs were sterilized by autoclave at 121°C. A mixture containing PAMPs and 25 μg/mL of BMP-2 (InductOS®, Wyeth/Pfizer, USA) in PBS was prepared. Subsequently, 200 μL of the solution was pipetted onto the BCP discs. The volume added was retained by the BCP discs without leakage. The final concentrations and dose per BCP disc are depicted in Table 1. The implants were air-dried overnight at room temperature and stored at 4°C until surgical implantation. All preparations were done in sterile conditions.

Animal experiment

The study involved 24 New Zealand White Rabbits (female, aged 20–25 weeks, Crl:KBL, Charles River, France). Ethical approval was granted by the local animal ethics committee at Utrecht University, The Netherlands, under the Central Authority for Scientific Procedures on Animals (license AVD1150002016445). The rabbits were housed in pairs at the Central Laboratory Animal Research Facility in Utrecht adhering to specified environmental parameters with food and water provided *ad libitum*. The animals' general well-being was assessed daily.

This study is the second procedure undergone by the animals. Five weeks prior, they underwent a posterolateral spinal fusion procedure, the details of which are reported elsewhere.[16] The animals demonstrated full recovery from the spinal surgery, as evident by baseline C-reactive protein (CRP) levels (Supplementary Fig. S2) and general well-being.

For the subcutaneous implantation surgery, animals received premedication with Buprenorphine (0.03 mg/kg, subcutaneous, Temgesic, Belgium) and a single administration of prophylactic antibiotic Penicillin (4×10^4 mg/kg s.c., Duplocilline®, Merck Animal Health, Canada). General anesthesia was induced with Midazolam (0.5 mg/kg, intramuscular), Etomidate (1.8 mg/kg, intravenous), and sustained with Sufentanyl (0.037 mg/kg) and Isoflurane (2–2.5 mL/h). The rabbit was placed in a prone position. The dorsal skin was shaved and disinfected with povidone-iodine. Ten subcutaneous pockets were created by making 1–2 cm incisions, spaced

Table 1. Experimental Groups of Implants

No.	*Groups*	*PAMP description*	*PAMP concentrations*		*BMP-2 (dose)*	n
1	Control	—	—	—	5 μg	24
2	*Bacillus Calmette-Guérin* (BCG)	Whole microbe	Hi	1×10^6 units/mL	5 μg	12
			Lo	1×10^5 units/mL	5 μg	12
3	γi-*S. aureus* (SA)	Whole microbe	Hi	1×10^6 units/mL	5 μg	12
			Lo	1×10^5 units/mL	5 μg	12
4	γi-*C. albicans* (CA)	Whole microbe	Hi	1×10^7 units/mL	5 μg	12
			Lo	1×10^5 units/mL	5 μg	12
5	Pam3CysSerLys4 (PAM)	Synthetic triacylated lipopeptide	Hi	10 μg/mL	5 μg	12
			Lo	0.1 μg/mL	5 μg	12
6	Curdlan	Exopolysaccharide	Hi	10 μg/mL	5 μg	12
			Lo	0.1 μg/mL	5 μg	12
7	CpG oligo-deoxynucleotide type C (CpG ODN C)	Analog of bacterial DNA	Hi	1 μg/mL	5 μg	12
			Lo	0.1 μg/mL	5 μg	12
8	Polyinosinic:polycytidylic acid (Poly[I:C])	Analog of viral RNA	Hi	10 μg/mL	5 μg	12
			Lo	0.1 μg/mL	5 μg	12
9	Peptidoglycan (PGN)	Gram-negative and positive bacterial cell wall component	Hi	10 μg/mL	5 μg	12
			Lo	0.1 μg/mL	5 μg	12
10	Lipopolysaccharide (LPS)	Gram-negative bacterial cell wall component	100 μg/mL		5 μg	12
11	Lipoteichoic acid (LTA)	Gram-positive bacterial cell wall component	3 mg/mL		5 μg	12
Total sample number						240

BMP-2, bone morphogenetic protein-2; PAMP, pathogen-associated molecular pattern.

approximately 4 cm apart. Implants were inserted into the pockets, and the incisions were closed with absorbable sutures (4.0 Monocryl®, Ethicon, USA).

A total of 24 animals were used, accommodating 240 subcutaneous pockets for implant placement. Each rabbit received 10 implants: 1 control implant (BMP-2 only), 1 implant with either LPS or LTA, and 8 implants containing high (Hi) and low (Lo) concentrations of four selected PAMPs (Fig. 1A). The four PAMPs for each rabbit were randomly chosen from a list of eight, according to a predefined randomization scheme (see Supplementary Table S1). Of the 240 total implants, 24 were control samples (one per animal), while each experimental group, representing a specific PAMP concentration, included 12 samples (Table 1).

To monitor adverse effects, blood CRP levels were measured before and after surgery (weeks 1 and 3), body temperature was monitored daily during the postsurgical week, and body weight was assessed weekly (Fig. 1B).

Fluorochrome labels were administered to determine the onset and direction of mineralization, with calcein green at week 2 (10 mg/kg subcutaneous, in 0.2 M $NaHCO_3$, Sigma-Aldrich) and xylenol orange at week 3 (30 mg/kg subcutaneous, in 0.12 M $NaHCO_3$, Sigma-Aldrich). After 5 weeks, euthanasia was carried out using a pentobarbital overdose (Euthanimal®, The Netherlands).

Tissue samples were harvested and fixed in 4% formaldehyde. Each implant was sectioned (1/4 and 3/4) using a circular saw (Dremel 4000, Mount Prospect, USA). One section (3/4) of the implant was embedded in methyl methacrylate (MMA, Merck Millipore, USA) for hard-tissue analysis to measure bone volume and detect fluorochrome signals. The remaining 1/4 of the implant was decalcified in 0.5 M EDTA and embedded in paraffin for osteoclast staining.

Bone histomorphometry

Undecalcified samples were used for histomorphometry. Briefly, samples were fixed in 4% (v/v) formaldehyde and dehydrated in an ethanol series (70%, 96%, and 100% ethanol). Afterward, the samples were incorporated into a mixture of MMA with 20% (v/v) plastoid N (Sigma-Aldrich) and 2.8% (w/v) benzoyl peroxide (Luperox, Sigma-Aldrich). Samples were immersed in a water bath at 37°C for 3 h to start polymerization. Four thin sections ($\sim$30 μm) were made from the middle region of each sample using a saw microtome (Leica, Nußloch, Germany). Two of the sections were stained with basic fuchsin and methylene blue, whereas the other two remained unstained for fluorochrome analysis. Stained sections were imaged (Olympus BX51 microscope), and the key structures including BCP scaffold, bone, and fibrous tissue were pseudo-colored using Adobe Photoshop 2020 (Adobe Systems, San Jose, USA). Bone tissue within the pore areas was quantified by calculating the proportion of bone pixels relative to the total pore area (expressed as bone area %). Noteworthy, bone marrow was excluded in this analysis. For each sample, an average of two sections was analyzed and quantified.

Fluorochrome detection

Fluorochrome signals were identified on unstained MMA-embedded samples. Signals were detected by fluorescence microscopy (Olympus BX51) using a duo block filter for fluorescein isothiocyanate/Texas red (dichroic mirror, 505/595 nm; Nikon, Japan) to observe calcein green (494/509–550 nm) and xylenol orange (570/610–780 nm).

Histology

A quarter of each sample was decalcified in 0.5 M EDTA and then embedded in paraffin and sectioned. For identification

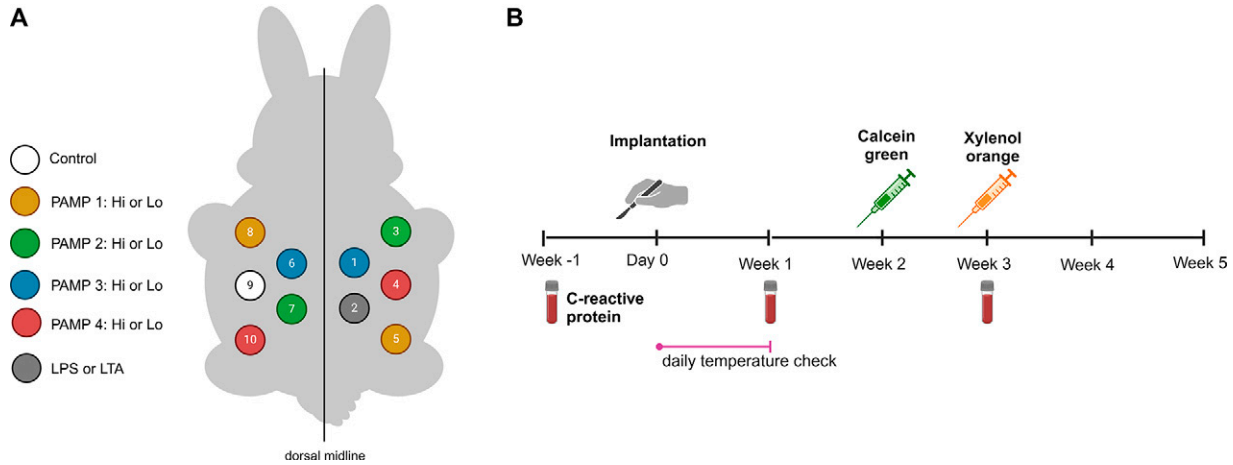

FIG. 1. Experimental setup. **(A)** The illustration depicts an example of the implants' randomization scheme. Ten subcutaneous pockets were made under the dorsal skin of each rabbit. Each animal received one control implant (only BMP-2), one implant with either LPS or LTA, and both a high (Hi) and low (Lo) concentration of four selected PAMPs. The four PAMPs were randomly chosen from a list of eight PAMPs according to a predefined randomization list. **(B)** Timeline of the subcutaneous implantations in rabbits. Fluorochromes (*calcein green and xylenol orange*) were administered on weeks 2 and 3 to detect mineralization onset. Monitoring for adverse effects was done by measuring C-reactive protein levels in the blood, body temperature in the first week after surgery, and weekly body weight. After 5 weeks of implantation, samples were harvested for analysis. Illustration created in https://BioRender.com. BMP-2, bone morphogenetic protein 2; LPS, lipopolysaccharide; LTA, lipoteichoic acid; PAMP, pathogen-associated molecular pattern.

of osteoclasts, samples were stained for tartrate-resistant acid phosphatase (TRAP). Briefly, samples were dewaxed, rehydrated, and then incubated in 0.2 M acetate buffer-tartaric acid (pH 5.0) for 20 min at room temperature. Afterward, they were immersed in a fresh solution of Naphtol AS-MX phosphate (0.5 mg/mL, Sigma-Aldrich) and Fast Red TR salt (1.1 mg/mL, Sigma-Aldrich) diluted in 0.2 M acetate buffer-tartaric acid (pH 5.0) for 1.5–2 h at 37°C. Then, the samples were rinsed and counterstained with Mayer's hematoxylin. Osteoclasts were identified as TRAP-positive multinucleated cells directly located on the surface of bone tissue or scaffold. Osteoclasts were identified as large or small, and when TRAP+ cells were lined adjacent with unclear borders, we arbitrarily counted them as two osteoclasts. Absolute numbers were counted for an average of two sections per sample. Results are reported as total cell count per area (number/mm^2).

Statistical analysis

The sample size calculation was performed for the primary outcome of this study; the relative difference in bone volume (bone area %) of the experimental group compared with the control informed by data from a prior study.[7] Power analysis was performed using G*Software (version 3.1.9.7, Germany) using the following parameters: F-tests (analysis of variance: fixed effect, special, main effects, and interactions), effect size (Cohen's) of 0.3536 (equivalent to d = 0.5), α of 0.05, and power of 0.80, for comparison of each experimental group to the control. A sample size of 10 animals per group was required. We increased this by 20% to account for potential missing data, which resulted in a final sample size of 12 per group.

Descriptive statistics are presented as proportion (%) and mean ± standard deviation (SD). Bone volume of the Hi and Lo concentrations of each PAMP was initially analyzed separately. Normality was assessed using the Shapiro–Wilk test, and differences were tested with the Mann–Whitney test. As no significant differences were found between Hi and Lo concentrations within any group, the data were pooled for both concentrations per PAMP to enhance statistical power for further analysis.

To normalize data distribution, Δbone area % was used as the parameter to compare the experimental groups (containing BMP-2 + PAMPs) to the control (BMP-2 only), where Δbone area % was calculated as the difference between the bone volume (bone area %) of an experimental group and the corresponding control within the same animal. A linear mixed model (LMM) with Benjamini–Hochberg[17] post hoc analysis was applied to assess the effect of PAMPs. The LMM included a fixed effect to estimate the average impact of the experimental groups on bone volume and random effects to account for variability among animals.

Osteoclast counts (number/mm^2) were presented as mean ± SD. Normality was assessed using the Shapiro–Wilk test, and differences in osteoclast count between groups of animals (nonresponders vs. responders) were tested with the Mann–Whitney test. All statistical analyses were performed using SPSS Statistics (version 29, IBM, USA) and figures created with GraphPad Prism 9 software (USA).

Results

Bone formation in the ectopic implants

The subcutaneous implantation of BCPs treated with the combination of low-dose BMP-2 and PAMPs did not lead to systemic adverse effects, as evidenced by stable CRP levels, body temperature, and weight throughout the study period (Supplementary Fig. S3). One animal failed to recover from the general anesthesia immediately after surgery and was therefore excluded from the study. Additionally, 7 implants (3%) out of the remaining 230 were found to partially or completely protrude from the skin during the healing process and therefore were not included in the analysis. In six animals, no ectopic bone was formed in any of the implants, and we further termed these animals as "nonresponders" (Fig. 2A). The number of implants per group included in the analysis is depicted in Table 2.

Table 2 shows the average bone volume in each group and the percentage of implants in which ectopic bone was present or not. In the control group (BMP-2 only), the average bone volume was 6.8% ± 8.5% with 59% of the implants showing the presence of ectopic bone and 41% not. In the experimental groups, ectopic bone was detected in >50% of implants in the PGN, BCG, and CpG ODN C group; ≤50% in the SA, CA, PAM, Poly(I:C), and LTA group; and no ectopic bone was detected in Curdlan and LPS group. Additionally, no differences in average bone volume were found between the implants with Hi and Lo concentration per PAMP (Supplementary Fig. S4). As a result, the data from both were pooled in the subsequent analysis to enhance statistical power.

Differences in bone volume between experimental groups and the control

Figure 2A depicts a paired dot plot that shows the bone volume of each implant treated with different PAMPs at both Hi and Lo concentrations, compared with its corresponding control implanted in the same animal. Most implants showed a negative or no change in bone volume compared with their respective control. Except for PGN, in which 9 out of 15 implants (60%) showed a positive change in bone volume compared with its relative controls.

Due to the large variations in bone volume (bone area %) within each group, the data were not distributed normally. To improve data distribution, Δbone area % was used as the parameter to compare PAMP groups and control. Δbone area% represents the difference in bone volume between the experimental implant and the control implant within each animal (Fig. 2B). Among the 10 PAMPs tested, PGN was the only group to show a positive mean in Δbone area % (+4.4%, $p = 0.08$) compared with the control. Decreased in bone volume was seen for Poly(I:C) (−6.30%, $p = 0.04$) and LPS (−7.4%, $p = 0.03$).

Histological analysis

The large variation in bone volume did allow for observation of the pattern, in which new bone formed inside BCP pores (Fig. 3A). More specifically, bone was typically found in a centrally located confined area inside the disc and never on the outside.

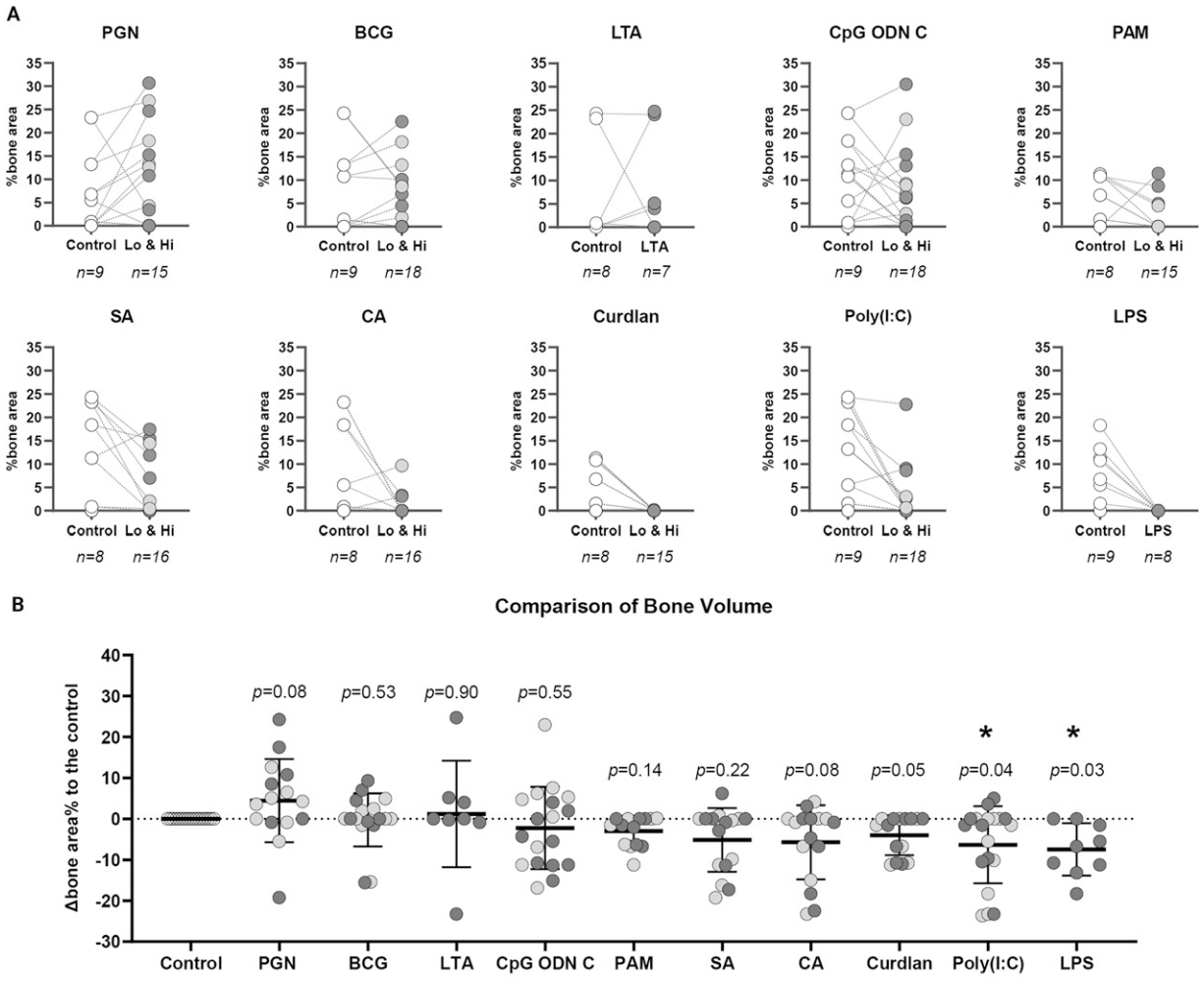

FIG. 2. The effect of PAMPs + BMP-2 (5 μg) on ectopic bone formation in BCP discs after 5 weeks of subcutaneous implantations in rabbits. **(A)** Paired dot plots showing bone volume (area %) from implants treated with different PAMPs at both Lo (*light gray*) and Hi (*dark gray*) concentrations, compared with its corresponding control. Dashed lines connect measurements from the same animal, and sample size (n) indicates the number of implants. Dots and lines may represent overlapping samples. **(B)** The percentage change of bone volume (Δbone area %) for the PAMP groups at both Lo (*light gray*) and Hi (*dark gray*) concentrations relative to their respective controls implanted within the same animal. Data are presented as mean ± SD. Statistical analysis was performed using the linear mixed model with Benjamini–Hochberg post hoc test (*$p < 0.05$). BCP, biphasic calcium phosphate; BMP-2, bone morphogenetic protein 2; PAMP, pathogen-associated molecular pattern; SD, standard deviation.

Basic fuchsin and methylene blue staining shows fibrous connective tissue and bone marrow filling the pores of the BCP with some bone tissue present (Fig. 3B). Bone tissue formed directly on the BCP surface, with cuboid osteoblasts visible on the newly formed bone. In several implants of the LPS group, the pores were infiltrated by numerous round, inflammatory cells.

TRAP staining shows multinucleated osteoclasts on the surface of BCP (Fig. 4A). The number of osteoclasts within the implants did not differ between the various PAMP groups. However, it was associated with whether an animal formed ectopic bone in the implants. Osteoclast numbers were significantly higher ($p = 0.004$) in implants retrieved from animals with ectopic bone present (responders; 17 animals) compared with those without ectopic bone in any implant (nonresponders; 6 animals; Fig. 4B).

Mineralization onset in ectopic implants

Fluorescent labels were administered to detect mineralization onset in the newly formed bone. Fluorescent signals were analyzed only in implants in which ectopic bone was present. We observed no signal for calcein green in any of the implants, indicating no mineralization to occur in the first 2 weeks after implantation. Positive signals were detected for xylenol orange (Fig. 4C) and were animal-dependent, irrespective of the different treatment groups. Of the 17 "responding animals," 47% showed positive signals (Fig. 4D)

Table 2. Bone Formation in Ectopic Implants

No.	*Group*	*Total implanted*	*Animals excluded*[a]	*Not retrieved*[b]	*Total remaining*	*Average bone volume (area % ±SD)*	*Ectopic bone present (%)*	*No ectopic bone (%)*
1	Control	24	7	—	17	6.8 ± 8.5	59	41
2	BCG							
	Hi	12	3	—	9	5.9 ± 7.4	56	44
	Lo	12	3	—	9	4.7 ± 6.9	56	44
3	γi-*S. aureus* (SA)							
	Hi	12	4	—	8	6.5 ± 7.5	50	50
	Lo	12	4	—	8	2.1 ± 5	38	63
4	γi-*C. albicans* (CA)							
	Hi	12	4	—	8	0.4 ± 1	13	88
	Lo	12	4	—	8	1.6 ± 3.4	25	75
5	Pam3CysSerLys4							
	Hi	12	4	—	8	3.1 ± 4.6	38	63
	Lo	12	4	1	7	0.6 ± 1.6	29	71
6	Curdlan							
	Hi	12	4	—	8	0	0	100
	Lo	12	4	1	7	0	0	100
7	CpG oligo-deoxynucleotide type C							
	Hi	12	3	—	9	8.1 ± 10	78	22
	Lo	12	3	—	9	5.6 ± 7.6	56	44
8	Polyinosinic:polycytidylic acid							
	Hi	12	2	2	8	5.4 ± 8	50	50
	Lo	12	2	—	10	0.4 ± 0.9	20	80
9	Peptidoglycan							
	Hi	12	4	1	7	12 ± 12	71	29
	Lo	12	4	—	8	9.4 ± 9.9	63	38
10	Lipoteichoic acid	12	4	1	7	5.9 ± 10.6	43	57
11	Lipopolysaccharide	12	3	1	8	0	0	100

[a]Excluded due to reaching the humane endpoint (one rabbit) and animals that did not form any ectopic bone (called nonresponders, six rabbits).
[b]Implants protruded outside the skin during the healing process and were not retrieved for analysis.
SD, standard deviation.

suggesting that mineralization onset occurred between 2 and 3 weeks after implantation. In the other 53%, ectopic bone formed after the 3rd week of implantation.

Discussion

PAMPs are potent immunomodulators that elicit a wide range of immune-stimulatory responses.[13] To determine whether PAMPs could function as osteoimmunomodulatory agents to enhance bone formation, we combined BCPs with different PAMPs and low-dose BMP-2. Implants were placed in the subcutaneous pockets of rabbits, with each animal receiving an internal control implant containing BMP-2 alone for comparison. After 5 weeks, our results showed minimal ectopic bone formation across the implants. No significant differences in bone volume were observed between the high and low concentrations of PAMPs. Among the PAMPs tested, PGN was the only group to exhibit a trend toward increased bone formation, although the effect size was modest, and with borderline significance. Only 60% of PGN-treated implants exhibited a positive response, indicating variability in its effect. Additionally, Poly(I:C) and LPS decreased bone volume compared with their relative controls. The variation in bone formation across animals suggests a degree of interindividual variability, as some animals did not form ectopic bone in any implants, including the BMP-2-only control.

Previous studies have explored the effects of whole microbes on *de novo* bone formation at skeletal[6,16] and extraskeletal (ectopic) locations.[7] At skeletal sites, different strains of nonviable bacteria including *S. aureus, E. coli*, and BCG (attenuated *M. bovis*) have induced a net increase in bone volume, suggesting a potential to promote bone formation under specific conditions.[6,16] However, the same microbial stimuli failed to promote bone formation at ectopic locations such as intramuscular and subcutaneous sites.[7] In a comparative study using different strains of nonviable bacteria, γi-*Haemophilus influenzae* (10^5–10^7 units/mL) was shown to promote bone formation when combined with BMP-2 (1.5 μg/mL) in BCP scaffolds after 8 weeks of implantation at subcutaneous sites in rabbits.[7] In contrast, other strains, including γi-*Bacillus cereus*, γi-*Escherichia coli*, γi-*Mycobacterium marinum*, and SA, showed no effect under similar conditions.[7,12] Likewise, in our study, SA, BCG, and CA did not induce ectopic bone formation.

Inconsistent findings were also observed with bacterial cell wall components in the subcutaneous implantations. Previous work has demonstrated that LTA (3 mg/mL), a Gram-positive cell wall component, promoted ectopic bone formation in BCP scaffolds when combined with lower-dose BMP-2 (1.5 μg/mL) in subcutaneous implants in rabbits after 8 weeks.[12] However, in our study, LTA at the same concentration failed to promote bone formation, suggesting a context-dependent effect. Several factors could contribute to this discrepancy, including implantation period, scaffold properties, BMP-2 dosage, and differences in host immune responses. These findings highlight the difficulty in comparing results across studies with different experimental parameters.

Different PAMPs induce distinct immune responses, yet a common feature is the activation of the canonical nuclear factor kappa B pathway, leading to the induction of proinflammatory mediators.[13] While inflammation is often associated with bone resorption in conditions such as osteoporosis and rheumatoid arthritis, its role in bone formation remains complex and context dependent.[18] Paradoxically, many of the mediators and signaling pathways implicated in pathological bone loss are also being studied in the pathogenesis of sporadic bone growth, for instance, in the case of heterotopic ossification (bone formation in soft tissue following trauma) and juvenile amputee overgrowth (excessive bone formation at amputation sites).[10,18] Deeper understanding of the biology underlying inflammation-mediated bone formation is essential to harness its potential for bone regeneration purposes.

The positive effects of microbial stimulation on bone volume are more frequently observed at skeletal locations compared with nonskeletal sites. One possible explanation is that skeletal tissues, particularly the periosteum, are highly responsive to inflammatory cues.[19] In adults, the osteogenic properties of the periosteum can be activated by trauma, infection, and growing tumors.[19] Cells within the periosteal layer, including osteoblasts and undifferentiated mesenchymal stem cells, respond by increasing their proliferation and differentiation activity, ultimately contributing to new bone formation.[20] A response is primarily regulated by inflammatory mediators and growth factors.[20] Given this, we propose that the cellular environment at skeletal locations provides a more favorable setting for inflammation-mediated bone regeneration.

We observed interindividual variations in ectopic bone formation across animals. We used the term "nonresponders" for animals in which no bone was present in any of the implants and the term "responders" for animals in which at least one implant showed ectopic bone formation. One possible explanation for this variability is differences in osteoclast activity. We observed a significantly higher number of osteoclasts in implants of the responder group compared with nonresponders ($p = 0.004$), aligning with previous reports linking increased osteoclast activity to enhanced *in vivo* bone regeneration.[21]

Several studies have investigated the role of osteoclasts in calcium phosphate (CaP) scaffolds. Evidence suggests that depleting osteoclast precursors, such as monocytes and macrophages, impaired bone formation at both extraskeletal[22–24] and skeletal sites.[25,26] Importantly, osteoclasts appear earlier

FIG. 3. Histology of undecalcified MMA-embedded sections. **(A)** Pseudo-coloring of implant sections shows the distribution of the different percentages of ectopic bone (*red*) in the pores (*purple*) of BCP (*gray*). **(B)** Basic fuchsin and methylene blue staining shows BCP scaffold (S, *dark brown*), bone tissue (B, *pink*), fibrous tissue (F, *purple*), and cuboid osteoblasts lining the surface of bone (*arrow*). In the LPS group, numerous round, nucleated cells (*, *dark purple*) are seen in the pores. Images are representative of implants with ectopic bone present (no ectopic bone was found for Curdlan and LPS). Scale bar: white =200 μm and yellow = 50 μm. BCP, biphasic calcium phosphate; LPS, lipopolysaccharide; MMA, methyl methacrylate.

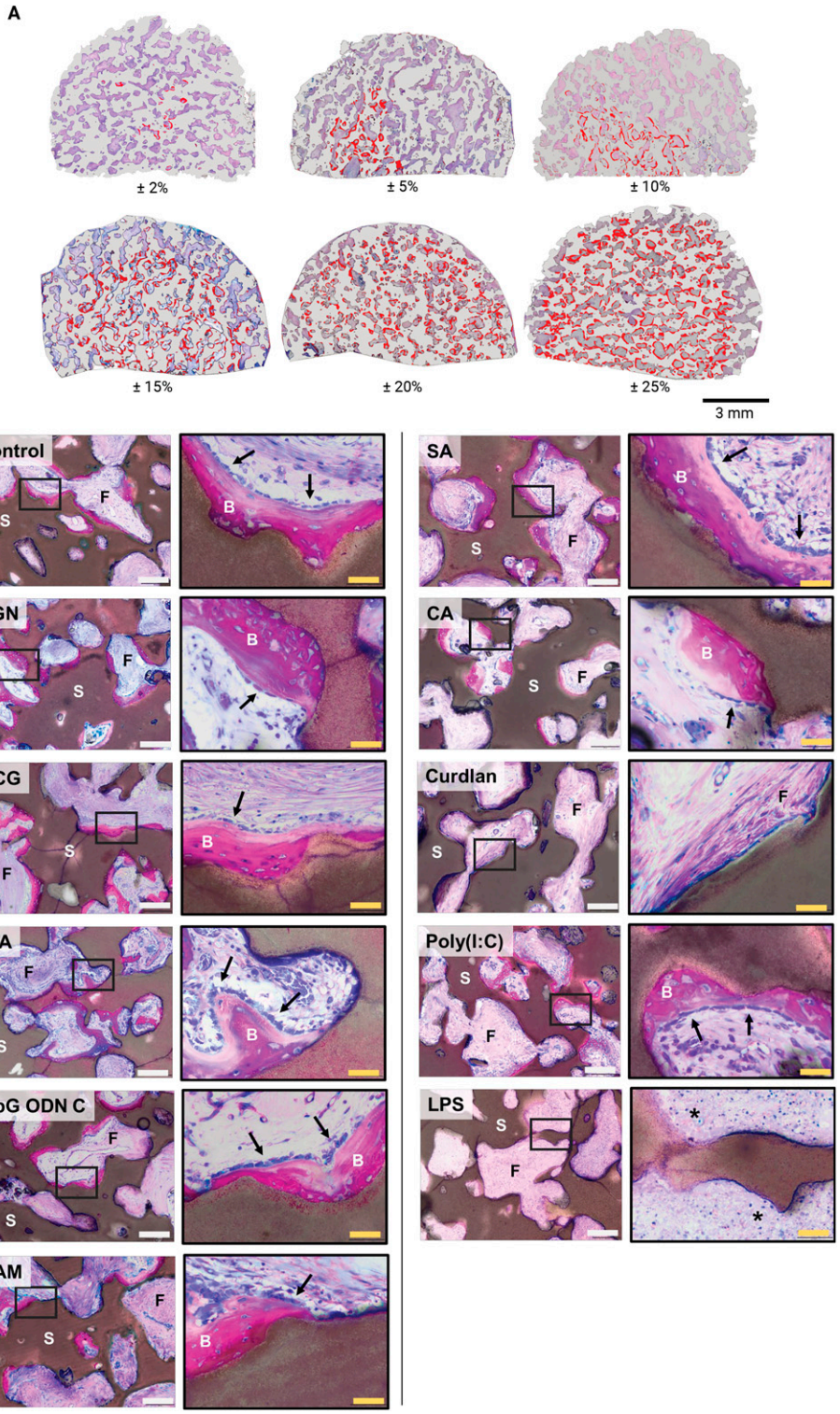

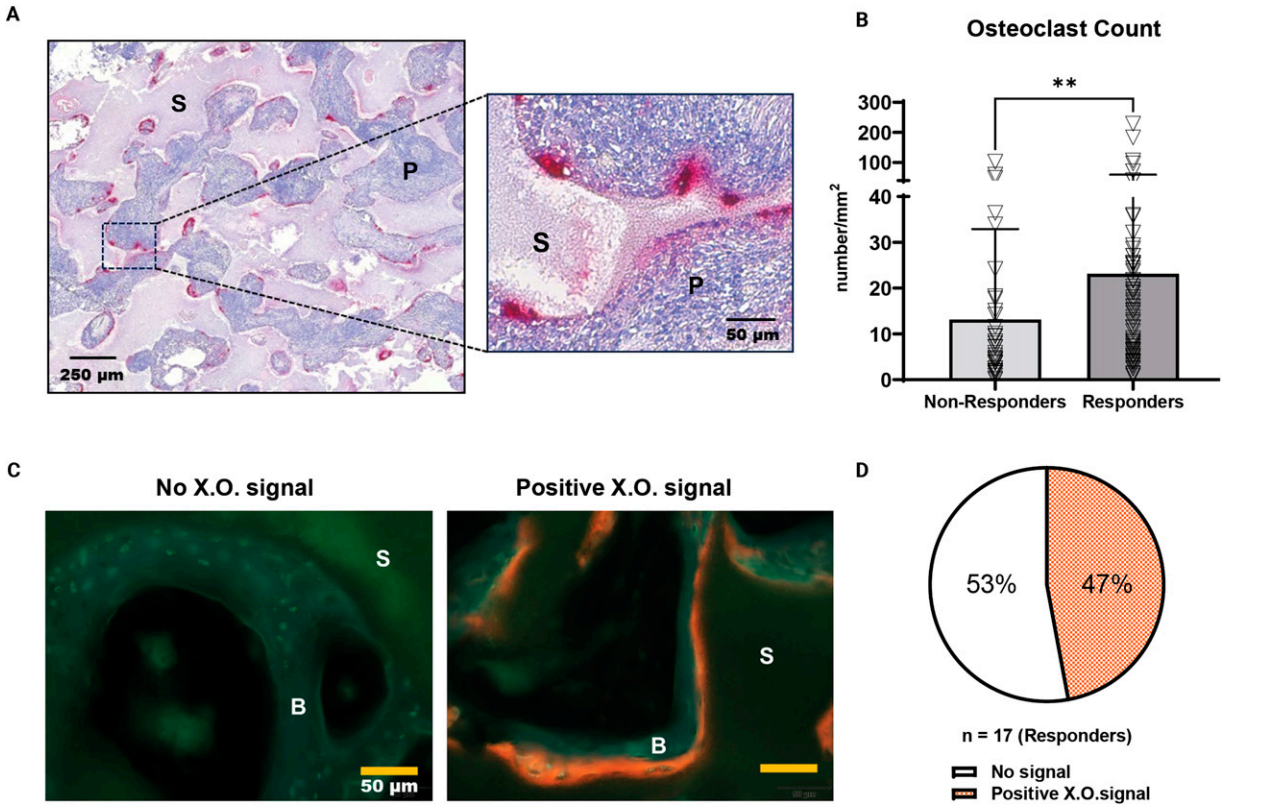

FIG. 4. Detection of osteoclasts and fluorescent labels. **(A)** TRAP staining on the decalcified sample shows osteoclasts (*red*) on the surface of BCP (S, *light purple*) and fibrous tissue filling the pores (P, *dark purple*). This image is representative of samples containing osteoclasts. **(B)** Osteoclast numbers were counted from implants retrieved from the nonresponders (animals with no ectopic bone in any implants; 6 animals) and responders (animals with at least one implant containing ectopic bone; 17 animals). Some data points may represent overlapping samples. Data are presented as mean ± SD. Statistical analysis was performed using the Mann–Whitney test; $^{**}p < 0.01$. **(C)** Fluorescent images showing the signal for xylenol orange (X.O., *orange line*) administered at week 3 but not calcein green administered at week 2. B = bone tissue, S = BCP scaffold. **(D)** The percentage of animals (responders, $n = 17$) with implants showing positive or no xylenol orange (X.O.) signal, irrespective of the treatment groups. BCP, biphasic calcium phosphate; SD, standard deviation; TRAP, tartrate-resistant acid phosphatase.

than osteoblasts in CaP implants.[24,25,27] Higher osteoclast activity has been associated with ectopic bone induction across species. For example, in a comparative study using similar CaP materials, ectopic bone formation occurred in dogs but not in rats, with a striking 600-fold difference in osteoclast numbers between the two species.[24] Supporting this, Li et al. found differences in the capacity of bone marrow macrophage to differentiate into osteoclasts among rat strains, identifying a strain in which ectopic bone formation can occur, and those that did not.[28] Our findings align with these reports, as higher osteoclast numbers were observed in animals that formed ectopic bone (Fig. 4B).

Several limitations should be considered. First, not all control group implants formed ectopic bone, which contrasts with earlier studies in rabbits, where ectopic bone was consistently present in scaffolds when BMP-2 was added.[7,12,14] In a pilot study (unpublished, $n = 5$) using the same experimental setup, mineralization in BCPs treated with 5 µg BMP-2 was observed between weeks 3 and 4 after implantation. Based on this, we applied a 5-week implantation period in the present study. However, our results showed considerable variation in bone formation (Table 2). Previous studies used a lower dosage of BMP-2 (1.5–3 µg) but a longer implantation period (8–12 weeks).[7,12] Future studies should explore longer implantation times to determine if this leads to more consistent bone formation outcomes.

Additionally, we used subcutaneous implant as the experimental unit rather than individual animals. While this design allows for multiple test groups per animal, it limits direct comparison of immune parameters between individual animals, as each rabbit received a unique combination of PAMPs. Exclusion of data from nonresponders and missing samples also reduced statistical power. However, since no significant differences were observed between the Hi and Lo PAMP concentrations, a pooled analysis remained feasible.

Conclusion

Our findings suggest that while PAMPs have the potential to modulate bone formation, their effects are variable, and further refinement is needed to harness their osteoimmunomodulatory properties effectively. In our model, PGN showed a positive trend in ectopic bone formation, whereas Poly(I:C) and LPS were associated with negative effects. However, variability in bone formation and the lack of statistical significance highlight the need for further validation studies. A more predictive *in vivo* model will be essential to

systematically evaluate PAMP effects, including dose–response relationships, different implantation locations, and extended implantation periods to create conditions more conducive to bone formation. A deeper understanding of the inflammatory profiles elicited by different PAMPs is also necessary to determine how immune stimulation can be fine-tuned to promote a controlled and beneficial inflammatory response. Additionally, osteoclast activity may play a role in interindividual variability, suggesting future studies should include parameters that assess osteoclast activities. While challenges remain, this study provides valuable insights that can inform the development of immune-targeted strategies for bone regeneration.

Authors' Contributions

N.R.R., M.C., and P.K. designed the experiments. N.R.R., A.A.A.D., M.C., and V.K. conducted the experiments, interpreted, and analyzed the data. N.R.R. wrote the article. M.C.K. and H.W. secured the funding and contributed to the experiment design, data interpretation, and article review. A.A.A.D. and D.G. contributed to data interpretation and article review. All authors have read and approved the final submitted article.

Ethical Approval

The animal experiment (protocol number AVD115 0002016445) was reviewed and approved by the Central Authority for Scientific Procedures on Animals (Centrale Commissie Dierproeven, the Netherlands) and by the local animal ethics committee (Instantie voor Dierenwelzijn, Utrecht, the Netherlands).

Author Disclosure Statement

No competing financial interests exist.

Funding Information

This work was supported by PPS allowance from the Health ~ Holland LSH-TKI (grant no.: LSHM18011) and the European Union's H2020 research and innovation program under Marie S. Curie Cofund RESCUE (grant agreement no. 801540).

Supplementary Material

Supplementary Figure S1
Supplementary Figure S2
Supplementary Figure S3
Supplementary Figure S4
Supplementary Table S1

References

1. Clarke B. Normal bone anatomy and physiology. Clin J Am Soc Nephrol 2008;3(Suppl 3):S131–S139; doi: 10.2215/CJN.04151206
2. Cypher TJ, Grossman JP. Biological principles of bone graft healing. J Foot Ankle Surg 1996;35(5):413–417; doi: 10.1016/S1067-2516(96)80061-5
3. Gillman CE, Jayasuriya AC. FDA-approved bone grafts and bone graft substitute devices in bone regeneration. Mater Sci Eng C Mater Biol Appl 2021;130:112466; doi: 10.1016/j.msec.2021.112466
4. Montoya C, Du Y, Gianforcaro AL, et al. On the road to smart biomaterials for bone research: Definitions, concepts, advances, and outlook. Bone Res 2021;9(1):12–16; doi: 10.1038/s41413-020-00131-z
5. Chen Z, Klein T, Murray RZ, et al. Osteoimmunomodulation for the development of advanced bone biomaterials. Mater Today 2016;19(6):304–321; doi: 10.1016/j.mattod.2015.11.004
6. Croes M, Boot W, Kruyt MC, et al. Inflammation-induced osteogenesis in a rabbit tibia model. Tissue Eng Part C Methods 2017;23(11):673–685; doi: 10.1089/ten.tec.2017.0151
7. Croes M, Kruyt MC, Boot W, et al. The role of bacterial stimuli in inflammation-driven bone formation. Eur Cell Mater 2019;37:402–419; doi: 10.22203/eCM.v037a24
8. Shi Y, Wang L, Niu Y, et al. Fungal component coating enhances titanium implant-bone integration. Adv Funct Materials 2018;28(46):1804483; doi: 10.1002/adfm.201804483
9. Rana RS, Wu JS, Eisenberg RL. Periosteal reaction. AJR Am J Roentgenol 2009;193(4):W259–W272; doi: 10.2214/AJR.09.3300
10. Bohner M, Miron RJ. A proposed mechanism for material-induced heterotopic ossification. Mater Today 2019;22:132–141; doi: 10.1016/j.mattod.2018.10.036
11. Li L, Jiang Y, Lin H, et al. Muscle injury promotes heterotopic ossification by stimulating local bone morphogenetic protein-7 production. J Orthop Translat 2019;18:142–153; doi: 10.1016/j.jot.2019.06.001
12. Croes M, Kruyt MC, Loozen L, et al. Local induction of inflammation affects bone formation. Eur Cell Mater 2017;33:211–226; doi: 10.22203/eCM.v033a16
13. Medzhitov R. Recognition of microorganisms and activation of the immune response. Nature 2007;449(7164):819–826; doi: 10.1038/nature06246
14. Croes M, Kruyt MC, Groen WM, et al. Interleukin 17 enhances bone morphogenetic protein-2-induced ectopic bone formation. Sci Rep 2018;8(1):7269; doi: 10.1038/s41598-018-25564-9
15. van Dijk LA, Barbieri D, Barrère-de Groot F, et al. Efficacy of a synthetic calcium phosphate with submicron surface topography as autograft extender in lapine posterolateral spinal fusion. J Biomed Mater Res B Appl Biomater 2019;107(6):2080–2090; doi: 10.1002/jbm.b.34301
16. Rahmani NR, Duits A, Croes M, et al. Incorporating microbial stimuli for osteogenesis in a rabbit posterolateral spinal fusion model. Tissue Eng Part A 2024; doi: 10.1089/ten.TEA.2024.0064
17. Benjamini Y, Hochberg Y. Controlling the false discovery rate: A practical and powerful approach to multiple testing. J R Stat Soc Ser B Methodol 1995;57(1):289–300.
18. Adamopoulos IE. Inflammation in bone physiology and pathology. Curr Opin Rheumatol 2018;30(1):59–64; doi: 10.1097/BOR.0000000000000449
19. Malizos KN, Papatheodorou LK. The healing potential of the periosteum: Molecular aspects. Injury 2005;36 (Suppl 3):S13–S19; doi: 10.1016/j.injury.2005.07.030
20. Lin Z, Fateh A, Salem DM, et al. Periosteum: Biology and applications in craniofacial bone regeneration. J Dent Res 2014;93(2):109–116; doi: 10.1177/0022034513506445
21. de Silva L, van den Beucken JJJP, Rosenberg AJWP, et al. Unraveling devitalization: Its impact on immune response and ectopic bone remodeling from autologous and allogeneic

callus mimics. Stem Cells Transl Med 2024;13(11): szae063–s1100; doi: 10.1093/stcltm/szae063
22. Davison NL, Gamblin AL, Layrolle P, et al. Liposomal clodronate inhibition of osteoclastogenesis and osteoinduction by submicrostructured beta-tricalcium phosphate. Biomaterials 2014;35(19):5088–5097; doi: 10.1016/j.biomaterials.2014.03.013
23. Davison NL, Su J, Yuan H, et al. Influence of surface microstructure and chemistry on osteoinduction and osteoclastogenesis by biphasic calcium phosphate discs. Eur Cell Mater 2015;29:314–329; doi: 10.22203/ecm.v029a24
24. Akiyama N, Takemoto M, Fujibayashi S, et al. Difference between dogs and rats with regard to osteoclast-like cells in calcium-deficient hydroxyapatite-induced osteoinduction. J Biomed Mater Res A 2011;96(2):402–412; doi: 10.1002/jbm.a.32995
25. Bighetti ACC, Cestari TM, Santos PS, et al. In vitro and *in vivo* assessment of CaP materials for bone regenerative therapy. The role of multinucleated giant cells/osteoclasts in bone regeneration. J Biomed Mater Res B Appl Biomater 2020;108(1):282–297; doi: 10.1002/jbm.b.34388
26. Tanaka T, Saito M, Chazono M, et al. Effects of alendronate on bone formation and osteoclastic resorption after implantation of beta-tricalcium phosphate. J Biomed Mater Res A 2010;93(2):469–474; doi: 10.1002/jbm.a.32560
27. Kondo N, Ogose A, Tokunaga K, et al. Osteoinduction with highly purified beta-tricalcium phosphate in dog dorsal muscles and the proliferation of osteoclasts before heterotopic bone formation. Biomaterials 2006;27(25):4419–4427; doi: 10.1016/j.biomaterials.2006.04.016
28. Li M, Li D, Jiang Y, et al. The genetic background determines material-induced bone formation through the macrophage-osteoclast axis. Biomaterials 2023;302:122356; doi: 10.1016/j.biomaterials.2023.122356

Address correspondence to:
Nada Ristya Rahmani, MD
Department of Orthopedics
University Medical Center Utrecht
Heidelberglaan 100
G05.228
Utrecht 3508 GA
The Netherlands

E-mail: n.r.rahmani@umcutrecht.nl

Received: January 16, 2025
Accepted: March 20, 2025
Online Publication Date: May 5, 2025